Peer-reviewed version available at *Water* **2018**, *10*, 1416; doi:10.3390/w10101416

Article

A Single Tube Contactor for Testing Membrane Ozonation

Garyfalia A. Zoumpouli [1,2], Robert Baker [1,2], Caitlin M. Taylor [1,2], Matthew J. Chippendale [2], Chloë Smithers [2], Sean H. S. Xian [2], Davide Mattia [2,3], Y.M. John Chew [2,3], and Jannis Wenk [2,3,*]

[1] Centre for Doctoral Training, Centre for Sustainable Chemical Technologies, University of Bath, BA2 7AY, UK; g.zoumpouli@bath.ac.uk (G.A.Z); r.baker@bath.ac.uk (R.B.); c.taylor2@bath.ac.uk (C.M.T.)

[2] Department of Chemical Engineering, University of Bath, BA2 7AY, UK; mjc83@bath.ac.uk (M.J.C.); cs897@bath.ac.uk (C.S.); sxh20@bath.ac.uk (S.H.S.X); d.mattia@bath.ac.uk (D.M.); y.m.chew@bath.ac.uk (Y.M.J.C.)

[3] Water Innovation and Research Centre (WIRC), University of Bath, BA2 7AY, UK

* Correspondence: j.h.wenk@bath.ac.uk; Tel.: +44-1225-38-3246

Abstract: A membrane ozonation contactor was built to investigate ozonation using tubular membranes and to inform computational fluid dynamics (CFD) studies. Non-porous tubular polydimethylsiloxane (PDMS) membranes of 1.0 – 3.2 mm inner diameter were tested at ozone gas concentrations of 110 – 200 g m^{-3} and liquid side velocities of 0.002 m s^{-1} – 0.226 m s^{-1}. The dissolved ozone concentration could be adjusted to up to 14 mg O_3 L^{-1} and increased with decreasing membrane diameter and liquid side velocity. Experimental mass transfer coefficients and molar fluxes of ozone were $1.1 \cdot 10^{-5}$ mol m^{-2} s^{-1} and $2.4 \cdot 10^{-6}$ m s^{-1}, respectively, for the smallest membrane. CFD modelling could predict the final ozone concentrations but slightly overestimated mass transfer coefficients and molar fluxes of ozone. Model contaminant degradation experiments and UV absorption measurements of ozonated water samples in both ozone (O_3) and peroxone (H_2O_2/O_3) reaction systems in pure water, river water, wastewater effluent and solutions containing humic acid show that the contactor system can be used to generate information on the reactivity of ozone with different water matrices. Combining simple membrane contactors with CFD allows predicting ozonation performance under a variety of conditions leading to improved bubble-less ozone systems for water treatment.

Keywords: ozonation; membranes; polydimethylsiloxane; mass transfer; wastewater treatment; peroxone.

1. Introduction

Ozone is a chemical oxidant used for water treatment for more than a century [1]. Ozone has a wide range of applications [2], including disinfection [3], control of disinfection byproducts [4,5], addressing taste and odor issues [6], and the removal of trace contaminants from both drinking water and during advanced wastewater treatment schemes [7-10]. Consequently, the usage of ozone has been steadily increasing for decades [11]. Ozone is an unstable gas that needs on-site production. The main costs for ozone operation are a combination of energy and oxygen consumption [12]. Usually, ozone is dissolved into the water phase via bubbling using various types of gas diffusers or side stream injection [13]. Knowledge and quantification of ozone mass transfer is crucial for the design of treatment operations [14]. Based on fundamental mass-transfer principles of gas-liquid systems ozone transfer is dependent on the interfacial area, the mass transfer coefficients, the solubility of gas in liquid and the concentration gradient between the gas and the liquid phase. In practice ozone transfer is also determined by the operating conditions such as mixing, the gas diffuser type, the water matrix and the setup of the treatment facility.

Bubble-less gas transfer by membranes permeable to ozone is an alternative to bubble-based methods [15]. Membrane contactors provide a constant interfacial surface area separating the gas phase from the liquid phase and result in readily predictable liquid flow patterns that enable

straightforward control over ozone gas to liquid mass transfer. The use of membranes may result in increased process efficiencies by significantly reducing off-gas disposal volume [16,17], and diminish practical challenges such as foaming issues [18]. The modular design of membrane contactors allows accurate responses to changing treatment needs and convenient maintenance. Particularly relevant for ozone applications is the targeted reduction of the regulated ozonation byproduct bromate that can be achieved when employing membrane contactors [19].

Despite obvious advantages and growing commercial interest for membrane ozonation the available literature on ozone transfer into water through membranes is comparatively small, with most studies focusing on ozone as a supplementary agent within hybrid treatment processes to increase membrane performance by reducing fouling or enhancing biodegradation of contaminants in membrane bioreactors (e.g. [20-22]).

Important attributes for ozonation membranes include porosity, surface hydrophobicity, selectivity for transfer of ozone over oxygen and stability during long-term ozone exposure. Ozone resistant inorganic ceramic membranes are made of alumina [23-25] and porous glass [26]. To prevent wetting of the surface and flooding of membrane pores, ceramic materials usually require surface modification to increase hydrophobicity [27-29]. Most polymeric membrane materials are hydrophobic but are prone to react with ozone. For example, polymers such as polyethersulfone (PES) and polyetherimide (PEI) possess carbon double bonds that react with ozone leading to decomposition [30]. Fluoropolymers such as polytetrafluoroethylene (PTFE) or polyvinylidene fluoride (PVDF) and polymers without functional groups exhibiting reactivity towards ozone such as plasticizer-free polydimethylsiloxane (PDMS) are more suitable for ozone [31]. Both PTFE and PDVF membranes have a sponge-like porous morphology and are resistant to ozone, while PDMS membranes have a dense non-porous morphology. Compared to fluoropolymers, PDMS is less resistant towards corrodants other than ozone, including UV [32-34]. Testing the long-term use of PDMS membranes in water treatment ozonation is still outstanding. However, given its availability in various sizes and its low purchase cost, PDMS appears as an appropriate model membrane material for smaller scale investigations of membrane ozonation processes.

In a previous study we developed a modelling approach based on computational fluid dynamics (CFD) and convection-diffusion theory to calculate ozone and oxygen gradients and their mass transfer through non-porous PDMS membranes into the aqueous phase [35]. The known material properties of PDMS and literature values on ozone mass transfer were used as input values for the model, while own experimental results were unavailable. The goal of this study was to create the experimental means to further verify and refine our modelling approach and enable data collection on ozonation experiments by using a simple ozone contactor system. Therefore, the objectives of this study were (i) to build a membrane contactor system as a flexible-use platform to investigate tubular membranes for ozonation, (ii) to measure the mass transfer of ozone into water through different PDMS membranes, (iii) to compare results with the previously developed model, and (iv) to conduct tests with established probe compounds for ozonation experiments in pure water, real water samples, and under peroxone process conditions by adding hydrogen peroxide (H_2O_2) to the aqueous phase.

2. Materials and Methods

All chemicals, including solvents and analytical consumables, were purchased from commercial sources: Potassium indigo trisulfonate (CAS 67627-18-3, Sigma-Aldrich), *para*-chlorobenzoic acid (*p*CBA, 99 % purity, Acros Organics), humic acid sodium salt (CAS 68131-04-4, technical grade, Sigma Aldrich), *N,N*-diethyl-p-phenylenediamine (DPD, 99 % purity, Acros Organics), peroxidase horseradish (≥ 85 units/mgdw, Alfa Aesar).

Ultrapure water (resistivity >18 MΩ/cm) was used for preparing stock solutions, analysis and experiments and was produced with Milli-Q (Merck) or ELGA (Veolia) water purification systems.

2.1. Membrane contactor system

Preprints (www.preprints.org) | NOT PEER-REVIEWED | Posted: 13 September 2018 doi:10.20944/preprints201809.0244.v1

Peer-reviewed version available at Water 2018, 10, 1416; doi:10.3390/w10101416

A schematic and a photograph of the lab-scale, single tube membrane contactor built for this study are shown in Figure 1. A borosilicate glass tube [length 20 cm, outer diameter (OD) 22 mm, inner diameter (ID) 18 mm] with two vertical and two horizontal screw connections (SQ24 and GL14, respectively) served as shell for the membrane contactor. Ozone resistant impermeable perfluoroalkoxy alkane (PFA) tubing (Swagelok, OD 1/8'') and Swagelok fittings (1/8'') made of 316 stainless steel were used for connecting both gas lines and liquid lines. The valves used were straight port HAM-LET H-800 ball valves (FTI Ltd, East Sussex, UK).

An ozone generator (BMT 803N, BMT Messtechnik GmbH, Berlin, Germany) fed with high purity oxygen (industrial grade, 99.5% purity, BOC, UK) was used to produce ozone (max. O_3 concentration > 250 g/Nm^3, or approx. 18% w/w). The oxygen flow rate was controlled with a rotameter (max. 300 mL/min, FLDO3306ST, Omega, Manchester, UK). The outlet of the ozone generator was connected to an ozone analyser (max. 200 g/m^3, BMT 964, BMT). The ozone/oxygen mixture was directed to the reactor through a plug valve. The gas mixture outlet was connected to a check valve (Swagelok) to prevent back flow, and then to a heated catalyst ozone to oxygen converter (CAT-RS, BMT). A purge line was included to flush the system off ozone when required.

The influent water was pumped using a diaphragm pump (0.25-20 mL/min, FMM 20 KPDC-P, KNF) and then directed to the reactor using a plug valve. The membrane tube ran through the center of the reactor. It was held in place at the two ends with silicone seals that provided leak-free operation. The membrane was connected to the liquid line outside the shell with push-on fittings. The water flow was from bottom to top, in counter-flow with the gas.

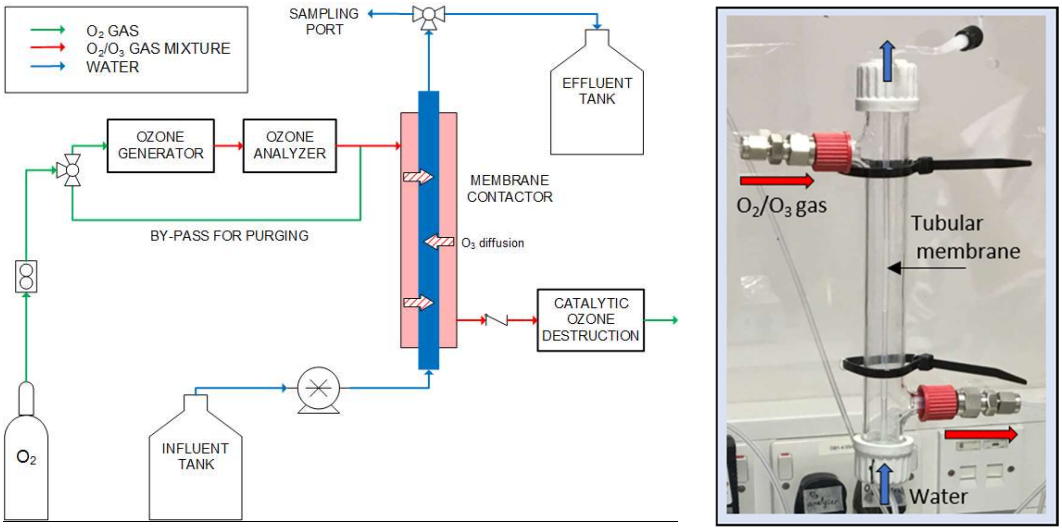

Figure 1. Schematic of the experimental setup and photograph of the membrane contactor.

2.2. Ozonation experiments

In all the experiments, the oxygen pressure was set to approximately 0.9 bar since the maximum operational pressure of the ozone generator was 1 bar. The oxygen flow rate was set to 100 mL/min. Experiments with different ozone concentrations in the gas phase were performed (7-14% weight O_3/weight gas mixture). The minimum concentration that could be achieved with the employed conditions was 110 g O_3/m^3 (±10%). The maximum ozone concentration was determined by the upper limit of the ozone analyzer and was 200 g O_3/m^3. The main characteristics of the PDMS membranes used are shown in Table 1. Except for membrane longevity tests, a new membrane was used for each experiment (i.e. after a few hours of use, the membrane was replaced).

The pump flow rate was measured at the beginning of each experiment using deionized water and a balance. Based on steady-state experiments, the system was left to stabilize for at least 10 minutes for flow rates between 5-20 mL/min, and for at least 20 minutes for flow rates less than 5 mL/min, before samples were taken.

Experiments were performed with different water matrices at room temperature (21°C ± 2°C): a) deionized water or phosphate buffer (pH=7.1), non-spiked, or spiked with *p*CBA (concentration approximately 10 µM) or humic acid (at various concentrations), b) secondary treated wastewater (wastewater effluent), or c) river water. For peroxone experiments, the influent was supplemented with 15-100 µM H_2O_2.

Table 1. PDMS tubing used in this study as non-porous membranes.

Material	Product code	Supplier	OD (in.)	ID (in.)	ID (mm)	Wall thickness (mm)
Silastic® (PDMS)	WZ-96115-22	Cole Parmer	1/4	1/8	3.2	1.6
Silastic® (PDMS)	WZ-96155-00	Cole Parmer	1/8	1/16	1.6	0.8
Silastic® (PDMS)	WZ-96115-08	Cole Parmer	1/12	1/25	1.0	0.6

2.3. Wastewater effluent and river water

Secondary treated wastewater was collected from a wastewater treatment plant in South-West England, UK. River water was collected from the River Avon in Bath, UK. For stabilization water samples were filtered with pre-rinsed glass microfiber filters grades GF/A or GF/C (nominal particle retention: 1.6 µm or 1.2 µm, respectively, Whatman, GE Life Sciences) and were stored at 4°C until used. Water sample properties and sampling dates are shown in Table 2.

Table 2. Water sample characteristics.

Property	Wastewater effluent (03/2018)	River water I (03/2018)	River water II (07/2017)
pH	7.9	7.2	8.2
TOC (mg/L)	10.2	7.2	4.3
UV_{254} (cm^{-1})	0.14	0.20	0.10
Alkalinity (mg $CaCO_3$/L)	181	236	n/a [1]
Nitrate (mg/L)	31	22	n/a

[1] n/a: not analyzed

2.4. Analytical methods

The concentration of dissolved ozone was measured with the indigo method [36]. The exact concentration of H_2O_2 in the feed water was measured with the DPD method [37]. UV-Vis measurements were performed with a UV-Vis spectrophotometer (Cary 100, Agilent Technologies) using 1 cm quartz glass cuvettes. The pH was measured with a pH meter (FE20, Mettler Toledo). The concentration of total organic carbon (TOC), as non-purgeable organic carbon (NPOC), was measured with a TOC analyzer (Shimadzu TOC 5000A). Alkalinity was determined by titration with 0.1 N hydrochloric acid according to ISO standard 9963-1:1994 [38]. Nitrate was measured with a HANNA® nitrate test kit (HI38050).

HPLC analysis of *p*CBA was performed with an Agilent HPLC System with a UV detector and an Acclaim RSLC 120 C18 column (3 µm, 120 Å, 3×75 mm). The mobile phase was 40 % acetonitrile and 60 % water with 10 mM phosphoric acid (pH=2.5). The flow rate was 0.5 mL/min and the injection volume was 50 µL. UV absorption was measured at 240 nm.

2.5. Computational modelling

Computational fluid dynamics (CFD) simulation is the generation of a numerical solution that satisfies a group of conservation equations (here, mass, momentum and species transport) over a computational domain that represents a real physical domain. The computational work was conducted using COMSOL Multiphysics V5.3 to determine the concentration profiles of O_3 (and O_2) in the gas, membrane, and liquid phase, so that major mass transfer resistances could be identified i.e. using a similar approach reported by Berry *et al.* (2017) [35]. The main difference, however, was the liquid and gas phase in this work were in the tube and shell side of the reactor respectively. The dimensions and operating conditions employed were those described in Section 2.2.

3. Results and Discussion

3.1. Ozone concentration with liquid side velocity and membrane size

The measured ozone concentrations at the outlet of the contactor compartment for the tested membranes at two different ozone gas concentrations and liquid side velocities ranging from 0.002 to 0.226 m/s are shown in Figure 2a. The corresponding modelled values are provided in Figure 2b, including Reynolds numbers and liquid side residence time (r.t.). The measured ozone concentration increased with smaller membrane diameter and decreasing liquid side velocity. Roughly doubling the ozone concentration from 110 g/m^3 to 200 g/m^3 in the gas phase resulted in higher dissolved ozone concentrations, especially for the thinner membranes.

Repetition experiments conducted with a different set of membrane tubes and different flow rates indicate good reproducibility and an experimental uncertainty of ±0.2 mg/L. In addition, experiments with a preliminary batch contactor setup showed that the relative standard deviation across different experiments was smaller than 10%; and is decreasing with membrane size. Better reproducibility with smaller membranes is ascribed to their faster response upon changes of experimental conditions. At higher liquid side flow rates and larger membrane size, some initial ozone bubble formation occurred along the inside of the membrane, but bubbles dispersed with equilibration. High flow rates caused non-uniform initial internal wetting of the membrane and created hydrophobic patches across the surface with lower resistance for ozone, leading to bubble formation. Both observations underline the importance for sufficient equilibration time at system startup and when altering experimental parameters.

Modelling results based on the previously developed CFD approach [35] agree with the experimental data. The relative deviation between modelling and experimental results was normally below 15%, although higher relative differences were occasionally observed for high liquid side velocities, as the model is not applicable to transitional and turbulent flows. Similarly, for low flow rates, i.e. for $Re \leq 100$, CFD slightly over-predicted the ozone concentration. A possible explanation for this disagreement is that at lower *Re* the dispersion of O_3 in the liquid phase is not uniform. Over the investigated range, this translates into an absolute deviation of less than 0.5 mg/L in the prediction of ozone concentrations, which is comparable to the experimental error of 0.2 mg/L. Generally, the modelled ozone concentration was higher than observed experimentally, indicating that the model slightly overestimates the actual ozone mass transfer.

Results confirm that liquid side velocity is the dominant parameter to determine the overall mass transfer of ozone followed by membrane thickness and ozone gas concentration. In practice, modules with bundles of thin membranes operating in parallel ensure low flow rates at large overall water fluxes to achieve required ozone concentrations [18]. Note that for data shown here both wall thickness and inner diameter simultaneously change based on the actual membrane dimensions (Table 2). Results for a hypothetical cylindrical membrane with constant inner diameter with increasing wall thickness are provided elsewhere [35].

Preprints (www.preprints.org) | NOT PEER-REVIEWED | Posted: 13 September 2018 doi:10.20944/preprints201809.0244.v1

Peer-reviewed version available at Water 2018, 10, 1416; doi:10.3390/w10101416

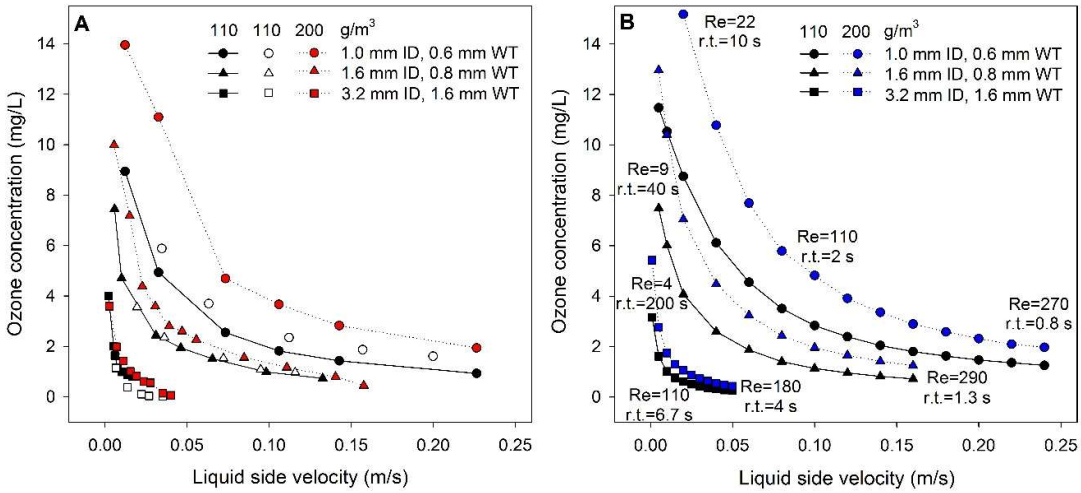

Figure 2. Dissolved ozone concentration in the outlet of the reactor against liquid velocity for different membranes diameters. A. Experimental results. Repeats (open symbols) were performed with a different set of membranes. B. CFD modeling results, including Reynolds numbers (Re) and liquid side residence times (r.t.).

3.2. Overall ozone mass transfer coeffiocients and molar fluxes through the membrane

To provide a better overview on mass transfer efficiency and an alternative comparison between experimental and modelling results, overall mass transfer coefficients K_L and molar fluxes of ozone were calculated.

The overall mass transfer coefficient was calculated according to equation (1):

$$\frac{K_L \alpha\, L}{u_L} = \frac{1}{H} ln \left\{ \frac{\frac{C_g}{S}}{\frac{C_g}{S} - HC_{L,out}} \right\}, \quad (1)$$

where α is the surface area of the membrane per unit volume of liquid, L is the length of the membrane, u_L is the liquid velocity, H is the solubility of ozone in water, S is the solubility of ozone in the PDMS membrane, C_g is the ozone concentration in the gas phase, and $C_{L,out}$ is the measured or calculated ozone concentration at the outlet of the contactor.

The molar flux of ozone across the membrane, N, was calculated according to equation (2):

$$N = K_L \left(\frac{C_g}{S} - HC_{L,out} \right), \quad (2)$$

The parameters used to calculate K_L and N are shown in Table 3. The overall mass transfer coefficients and the molar fluxes of ozone for the three tested membranes are shown in Figure 3. Error bars for experimental data were determined using error propagation based on the uncertainties shown in Table 3. It is expected that the effect of inlet O_3 concentration on K_L is insignificant since it largely depends on the hydrodynamics (Re) and transport properties of O_3 in water, in particular the Schmidt number (Sc) [35], which is the ratio of momentum diffusivity and mass diffusivity). In contrast, N is strongly dependent on the inlet concentration, which directly affects the concentration gradient. Values of N for 200 g/m^3 can be expected about twice that of 110 g/m^3.

Table 3. Parameters used for calculation of K_L and N.

Property	Units	Value	Experimental uncertainty (±)	Reference
α	m^{-1}	4000 (1.0 mm ID) 2500 (1.6 mm ID) 1250 (3.2 mm ID)	-	calculated
L	m	0.2	-	contactor length
u_L	m/s	0.002-0.224	0.002	calculated
H	-	0.248	-	[39]
S	-	0.881	-	[40]
C_g	mol/m^3	2.1-2.5	0.2	measured
$C_{L,out}$	mol/m^3	0.014-0.186	0.004	measured (experimental) or calculated (modelled)

Mass transfer coefficients and molar fluxes increase with increasing liquid side velocity and level off at higher velocities, while dissolved ozone concentration decreases with increasing velocity, as discussed in the previous section. This agrees with both experimental and computational studies employing membranes made of different materials [31,35,41,42]. In addition, the mass transfer coefficients calculated for PDMS are of the same order of magnitude than those reported for porous fluoropolymer membranes. For example, for PTFE and PVDF flat sheet membranes at Re = 60 the mass transfer coefficients of ozone ranged from 5.4×10^{-6} m/s to 1.1×10^{-5} m/s [31], while in a hollow fiber PVDF membrane module the mass transfer coefficients ranged from 5.30×10^{-7} to 1.84×10^{-5} m/s for liquid side velocities ranging from 0.01 to 0.5 m/s [41].

Mass transfer coefficient and molar flux data confirm the already discussed overestimation of ozone mass transfer by the modelling approach, which is beyond the experimental error margin. The discrepancy between modelling and experimental results appears more pronounced using the data representation of Figure 3, while the differences in actual ozone concentrations are modest from an application viewpoint. The experimental uncertainty increases for larger diameters due to the larger relative error on measured ozone concentration. In addition, at higher velocities experimental results show a decrease in both molar flux and mass transfer coefficient, which is different, compared to model results and associated to much longer equilibration times needed to achieve constant gas transfer conditions for these membrane diameters.

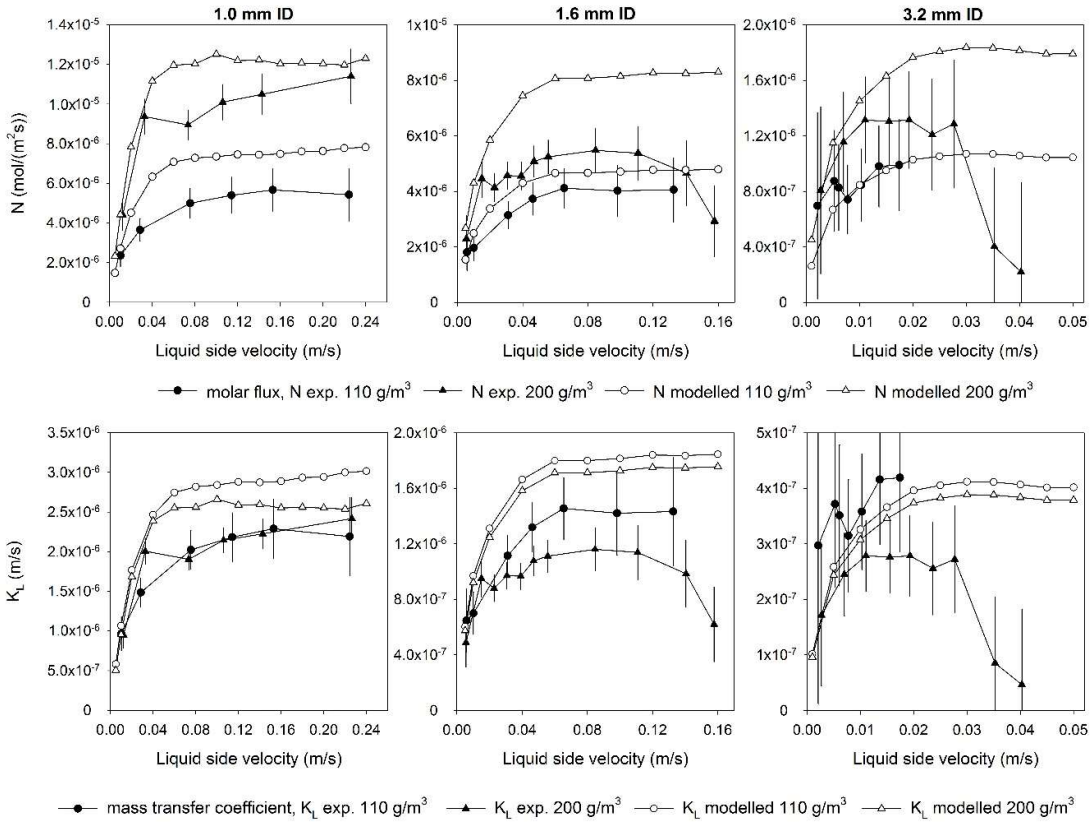

Figure 3. Experimental and modelled overall mass transfer coefficients K_L and molar fluxes of ozone N at ozone gas concentration of 110 g/m³ and 200 g/m³ versus liquid side velocity.

3.3. Removal of pCBA by membrane ozonation and in presence of additional H_2O_2 (peroxone process)

Ozone decomposition in water results in the formation of the OH radical, the major secondary oxidant during ozonation [43]. In contrast to ozone which is a selective oxidant, OH radicals are short lived and undergo fast reaction with most organic reactants [44]. Therefore, OH radicals play an important role in the removal of organic contaminants during ozonation because they effectively transform any organic contaminant present in water at similar reaction rates [45], while disinfection mainly occurs through ozone directly.

To assess OH radical-induced oxidation processes in the experimental setup, the removal of the ozone-resistant OH radical probe [46] and established model trace contaminant compound *p*CBA [47] was determined for different membrane thicknesses. Experiments were also conducted by adding H_2O_2. The reaction of hydrogen peroxide with ozone (peroxone process) creates an increased OH radical concentration [48]. The peroxone process has been widely used to improve treatment efficiency for compounds that react slowly with ozone [49].

Figure 4a shows the removal of *p*CBA in pure water for different liquid side velocities and membrane thicknesses. As expected and based on ozone concentration measurements (section 3.1), the *p*CBA removal increased with residence time and with decreasing membrane thickness. Note that liquid side chemical reactions promote ozone transfer, by increasing the concentration gradient across the membrane. To determine accurate mass transfer, an enhancement factor has to be considered that depends on the reaction kinetics of the target contaminants with ozone and its oxidative decomposition products[50].

The added H_2O_2 concentration to achieve an O_3:H_2O_2 ratio of 2:1 on a molar basis [48,51] was 15 µM (0.5 mg H_2O_2/L) and was calculated for the ozone transferred in pure water under the tested experimental conditions (1.6 mm ID membrane, v = 0.07 m/s, residence time 3 s), which was approximately 31 µM (1.5 mg O_3/L). A higher H_2O_2 concentration of 100 µM was also tested. In pure buffered water the addition of H_2O_2 did not lead to a significant increase in *p*CBA removal (Figure 4a). Similar results have been observed in a membrane contacting system employing a ceramic membrane, where the peroxone process increased the removal of *p*CBA in river water by less than 10 % [52]. A higher improvement of *p*CBA removal has been observed by H_2O_2 addition in batch experiments [48,53]. The difference between the conventional (batch) peroxone process and the membrane peroxone process can be attributed to the non-uniform concentration of ozone in the membrane, which influences the O_3:H_2O_2 ratio and thus the OH radical yield [52].

The higher H_2O_2 concentration tested did not have a significant additional effect. Measurements of the residual ozone concentration confirmed that the ozone consumption was very similar for both H_2O_2 concentrations. For lower flow rates (residence time more than 3 s) the ozone consumption was incomplete, due to the higher ozone concentration. In a PTFE hollow fiber module the increase of H_2O_2 concentration led to an increase in *p*CBA removal, but the experiments were performed with longer residence times and lower ozone gas concentrations [19].

The removal of *p*CBA in different types of water (Figure 4b) and a humic acid solution was lower than in pure water due to the presence of matrix compounds that act as OH radical and ozone scavengers (Table 2). With the addition of 15µM H_2O_2 the *p*CBA removal showed a small increase in all four water matrices tested.

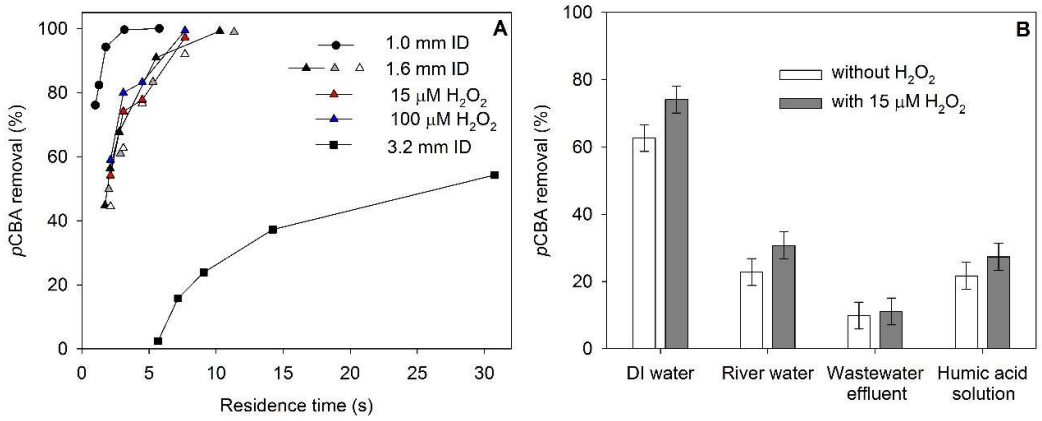

Figure 4. A. Removal of *p*CBA in pure buffered water and with added H_2O_2 for different membrane sizes. Repeats performed with a different membrane each time are shown for the 1.6 mm ID membrane. B. Removal of *p*CBA in different water matrices, with and without addition of H_2O_2 for 1.6 mm ID membranes. TOC concentrations were 7.2, 10.2, and 8.3 for River Water I, wastewater effluent and humic acid solution, respectively, at a residence time of three seconds.

3.4. Ozonation of dissolved organic matter

The effect of ozone on the dissolved organic matter present in the three different water matrices (river water, wastewater effluent and humic acid solution) was determined by measuring UV_{254} absorption before and after passage through the membrane module. Figure 5A provides relative changes in UV_{254} and residual ozone concentrations plotted against TOC concentration. For humic acid, the change in absorption decreases with increasing TOC concentration, along with a decrease in residual ozone concentration. From 3 mg/L TOC, no further reduction of the residual concentration of ozone can be observed due to the short residence time of four seconds in the reactor. At the same

Preprints (www.preprints.org) | NOT PEER-REVIEWED | Posted: 13 September 2018 doi:10.20944/preprints201809.0244.v1

Peer-reviewed version available at Water 2018, 10, 1416; doi:10.3390/w10101416

TOC, river water shows both a greater decrease in absorption (24%) and a higher residual ozone concentration (0.7 mg/L) than humic acid solution. This indicates that the tested river water is less reactive with ozone, whereas the results for wastewater effluent are comparable to those for humic acid, indicating a high reactivity with ozone. Figure 5B gives the change in absorption at different liquid side velocities for river water and wastewater effluent. At higher liquid side velocities, the change in absorption decreases due to the lower ozone exposure. Overall, the results for section 3.3 and 3.4 show that the single membrane ozonation experiments can be used to obtain information on the reactivity of the water matrix with ozone with relatively modest experimental effort as, for example, ozone exposure can be controlled via liquid side velocities.

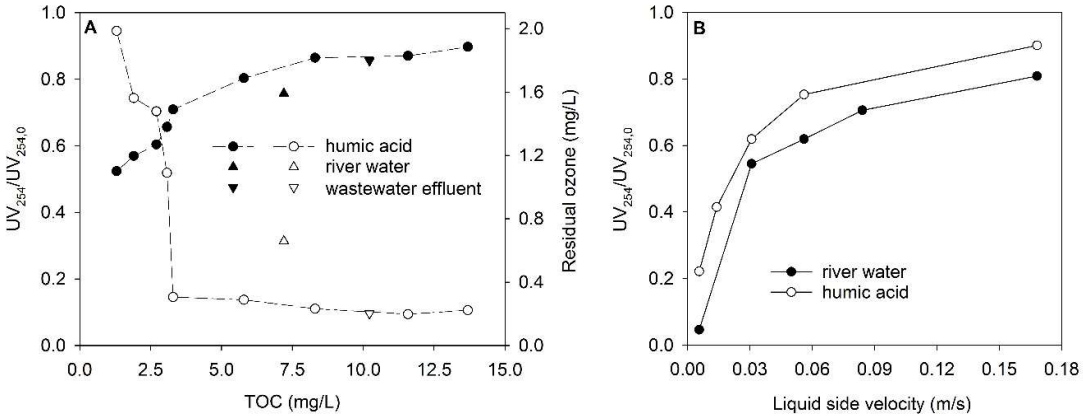

Figure 5. A. Relative change in UV_{254} absorbance (closed symbols) and residual ozone concentration (open symbols) for river water I, wastewater effluent and humic acid solutions at different TOC, 1.6 mm ID membrane, 4 s residence time, ozone gas concentration 110 g/m^3. B. Relative change in UV_{254} absorbance at different liquid side velocity for river water II (TOC 4.3 mg/L) and humic acid (TOC 3.6 mg/L) for a 1.6 mm ID membrane and 200 g/m^3 ozone gas concentration.

3.5. Membrane longevity

During repeated use of membranes over several months in a preliminary batch setup and continuous ozonation experiments over 12 hours with wastewater effluent and 24 hours with pure water no signs of fatigue of membranes was noticed. However, a slight increase in TOC of water samples after contactor passage, which was detectable but within the analytical error, was found. Ozone exposure induces structural modifications on PDMS [30,32]. Ozone and UV combined oxidize PDMS to form SiO_x, by substituting methyl groups with hydroxyl groups [34,54,55] and ozone in the presence of water leads to formation of peroxides on the PDMS surface [56]. The effect of ozone on PDMS, including aging, has no implications for the data presented in this work, but should be considered when planning experimental studies.

4. Conclusions

A single tube ozonation contactor was successfully built and tested with non-porous PDMS membranes. The overall mass transfer coefficient and molar flux of ozone were found to increase with increasing liquid side velocity and to level off at higher velocities. Comparing results with a previously developed computational mass transfer model showed good agreement to predict final ozone concentrations. The experimental and computational results also showed that concentration of ozone in the gas phase on the overall mass transfer is insignificant. Three different types of water were tested to investigate the effect of the water matrix, including different TOC levels on the

degradation of a model compound under ozone and peroxone conditions. Single tube systems can be used to test different types of membranes. The integration of computational and experimental studies is a powerful tool to inform the design of membrane ozone contactors.

Acknowledgments: Financial support for undergraduate research projects of C.S. and M.J.C. by the Department of Chemical Engineering and start-up infrastructure funding by the Faculty of Engineering & Design for J.W. is appreciated. S.H.S.X. was supported by an Institute for Mathematical Innovation (IMI) undergraduate research internship. C.M.T., G.A.Z and R.B. were supported by EPSRC funded integrated Ph.D. studentships in Sustainable Chemical Technologies (EP/L016354/1). G.A.Z. was also supported by a University of Bath research scholarship. This research was supported by a Royal Society equipment grant (RG2016-150544).

Author Contributions: Y.M.J.C.; D.M. and J.W. conceived and designed the study; R.B. built the contactor system; C.M.T., R.B., G.A.Z., C.S. and M.J.C. conducted sampling, experiments and analysis, S.H.S.X. and Y.M.J.C performed the computational fluid dynamics modelling, G.A.Z. and J.W. interpreted the results; G.A.Z. and J.W. conducted the literature research; G.A.Z, Y.M.J.C. and J.W. wrote the paper.

Conflicts of Interest: The authors declare no conflict of interest.

Abbreviations

Nomenclature

α	surface area of the membrane per unit volume of liquid	m^{-1}
L	length of the membrane	m
u_L	liquid velocity	m/s
H	solubility of ozone in water	-
S	solubility of ozone in the membrane	-
C_g	ozone concentration in the gas phase	g/m^3
$C_{L,out}$	ozone concentration at the outlet of the contactor	mg/L
K_L	Overall mass transfer coefficient	m/s
N	Molar flux	$mol/(m^2\ s)$
Re	Reynolds number	-
Sc	Schmidt number	-

Acronyms

CFD	Computational fluid dynamics
PDMS	Polydimethylsiloxane
PES	Polyethersulfone
PEI	Polyetherimide
PFA	Perfluoroalkoxy alkane
PTFE	Polytetrafluoroethylene
PVDF	Polyvinylidene difluoride
DPD	*N,N*-diethyl-p-phenylenediamine
*p*CBA	*para*-chlorobenzoic acid
ID	inner diameter
OD	outer diameter

TOC total organic carbon

References

1. Le Paulouë, J.; Langlais, B. State-of-the-art of ozonation in france. *Ozone: Science & Engineering* **1999**, *21*, 153-162.
2. von Gunten, U. Oxidation processes in water treatment: Are we on track? *Environ Sci Technol* **2018**, *52*, 5062-5075.
3. Gottschalk, C.; Libra, J.A.; Saupe, A. *Ozonation of water and waste water: A practical guide to understanding ozone and its applications*. John Wiley & Sons: 2009.
4. Chuang, Y.-H.; Mitch, W.A. Effect of ozonation and biological activated carbon treatment of wastewater effluents on formation of n-nitrosamines and halogenated disinfection byproducts. *Environmental Science & Technology* **2017**, *51*, 2329-2338.
5. Hua, G.; Reckhow, D.A. Comparison of disinfection byproduct formation from chlorine and alternative disinfectants. *Water Research* **2007**, *41*, 1667-1678.
6. Nakamura, H.; Oya, M.; Hanamoto, T.; Nagashio, D. Reviewing the 20 years of operation of ozonation facilities in hanshin water supply authority with respect to water quality improvements. *Ozone: Science & Engineering* **2017**, *39*, 397-406.
7. Camel, V.; Bermond, A. The use of ozone and associated oxidation processes in drinking water treatment. *Water Research* **1998**, *32*, 3208-3222.
8. Snyder, S.A.; Wert, E.C.; Rexing, D.J.; Zegers, R.E.; Drury, D.D. Ozone oxidation of endocrine disruptors and pharmaceuticals in surface water and wastewater. *Ozone: Science & Engineering* **2006**, *28*, 445-460.
9. Loeb, B.L.; Thompson, C.M.; Drago, J.; Takahara, H.; Baig, S. Worldwide ozone capacity for treatment of drinking water and wastewater: A review. *Ozone: Science & Engineering* **2012**, *34*, 64-77.
10. Bourgin, M.; Beck, B.; Boehler, M.; Borowska, E.; Fleiner, J.; Salhi, E.; Teichler, R.; von Gunten, U.; Siegrist, H.; McArdell, C.S. Evaluation of a full-scale wastewater treatment plant upgraded with ozonation and biological post-treatments: Abatement of micropollutants, formation of transformation products and oxidation by-products. *Water Research* **2018**, *129*, 486-498.
11. Loeb, B.L. Forty years of advances in ozone technology. A review of ozone: Science & engineering. *Ozone: Science & Engineering* **2018**, *40*, 3-20.
12. Mundy, B.; Kuhnel, B.; Hunter, G.; Jarnis, R.; Funk, D.; Walker, S.; Burns, N.; Drago, J.; Nezgod, W.; Huang, J., *et al.* A review of ozone systems costs for municipal applications. Report by the municipal committee – ioa pan american group. *Ozone: Science & Engineering* **2018**, *40*, 266-274.
13. Rakness, K.L.; Hunter, G.; Lew, J.; Mundy, B.; Wert, E.C. Design considerations for cost-effective ozone mass transfer in sidestream systems. *Ozone: Science & Engineering* **2018**, *40*, 159-172.
14. Zhou, H.; Smith, D.W. Ozone mass transfer in water and wastewater treatment: Experimental observations using a 2d laser particle dynamics analyzer. *Water Research* **2000**, *34*, 909-921.
15. Basile, A.; Cassano, A.; Rastogi, N.K. *Advances in membrane technologies for water treatment: Materials, processes and applications*. 2015; p 1-342.
16. Zhou, H.; Smith, D.W. Ozonation dynamics and its implication for off-gas ozone control in treating pulp mill wastewaters. *Ozone: Science & Engineering* **2000**, *22*, 31-51.
17. Oneby, M.A.; Bromley, C.O.; Borchardt, J.H.; Harrison, D.S. Ozone treatment of secondary effluent at u.S. Municipal wastewater treatment plants. *Ozone: Science & Engineering* **2010**, *32*, 43-55.
18. Gabelman, A.; Hwang, S.-T. Hollow fiber membrane contactors. *Journal of Membrane Science* **1999**, *159*, 61-106.

19. Merle, T.; Pronk, W.; von Gunten, U. Membro3x, a novel combination of a membrane contactor with advanced oxidation (o3/h2o2) for simultaneous micropollutant abatement and bromate minimization. *Environmental Science & Technology Letters* **2017**, *4*, 180-185.
20. Van Geluwe, S.; Braeken, L.; Van der Bruggen, B. Ozone oxidation for the alleviation of membrane fouling by natural organic matter: A review. *Water Research* **2011**, *45*, 3551-3570.
21. Kim, J.; Davies, S.H.R.; Baumann, M.J.; Tarabara, V.V.; Masten, S.J. Effect of ozone dosage and hydrodynamic conditions on the permeate flux in a hybrid ozonation–ceramic ultrafiltration system treating natural waters. *Journal of Membrane Science* **2008**, *311*, 165-172.
22. Laera, G.; Cassano, D.; Lopez, A.; Pinto, A.; Pollice, A.; Ricco, G.; Mascolo, G. Removal of organics and degradation products from industrial wastewater by a membrane bioreactor integrated with ozone or uv/h2o2 treatment. *Environmental Science & Technology* **2012**, *46*, 1010-1018.
23. Stylianou, S.K.; Sklari, S.D.; Zamboulis, D.; Zaspalis, V.T.; Zouboulis, A.I. Development of bubble-less ozonation and membrane filtration process for the treatment of contaminated water. *Journal of Membrane Science* **2015**, *492*, 40-47.
24. Wenten, I.G.; Julian, H.; Panjaitan, N.T. Ozonation through ceramic membrane contactor for iodide oxidation during iodine recovery from brine water. *Desalination* **2012**, *306*, 29-34.
25. Janknecht, P.; Picard, C.; Larbot, A.; Wilderer, P.A. Membrane ozonation in wastewater treatment. *Acta Hydroch. Hydrob.* **2004**, *32*, 33-39.
26. Kukuzaki, M.; Fujimoto, K.; Kai, S.; Ohe, K.; Oshima, T.; Baba, Y. Ozone mass transfer in an ozone–water contacting process with shirasu porous glass (spg) membranes—a comparative study of hydrophilic and hydrophobic membranes. *Sep. Purif. Technol.* **2010**, *72*, 347-356.
27. Stylianou, S.K.; Szymanska, K.; Katsoyiannis, I.A.; Zouboulis, A.I. Novel water treatment processes based on hybrid membrane-ozonation systems: A novel ceramic membrane contactor for bubbleless ozonation of emerging micropollutants. *Journal of Chemistry* **2015**, *2015*, 1-12.
28. Mosadegh-Sedghi, S.; Rodrigue, D.; Brisson, J.; Iliuta, M.C. Wetting phenomenon in membrane contactors – causes and prevention. *Journal of Membrane Science* **2014**, *452*, 332-353.
29. Zhang, Y.; Li, K.; Wang, J.; Hou, D.; Liu, H. Ozone mass transfer behaviors on physical and chemical absorption for hollow fiber membrane contactors. *Water Science and Technology* **2017**, *76*, 1360-1369.
30. Santos, F.R.A.d.; Borges, C.P.; Fonseca, F.V.d. Polymeric materials for membrane contactor devices applied to water treatment by ozonation. *Materials Research* **2015**, *18*, 1015-1022.
31. Pines, D.S.; Min, K.-N.; Ergas, S.J.; Reckhow, D.A. Investigation of an ozone membrane contactor system. *Ozone: Science & Engineering* **2005**, *27*, 209-217.
32. Shanbhag, P.V.; Sirkar, K.K. Ozone and oxygen permeation behavior of silicone capillary membranes employed in membrane ozonators. *J. Appl. Polym. Sci.* **1998**, *69*, 1263-1273.
33. Shanbhag, P.V.; Guha, A.K.; Sirkar, K.K. Membrane-based ozonation of organic compounds. *Industrial & Engineering Chemistry Research* **1998**, *37*, 4388-4398.
34. Ouyang, M.; Yuan, C.; Muisener, R.J.; Boulares, A.; Koberstein, J.T. Conversion of some siloxane polymers to silicon oxide by uv/ozone photochemical processes. *Chem. Mater.* **2000**, *12*, 1591-1596.
35. Berry, M.; Taylor, C.; King, W.; Chew, Y.; Wenk, J. Modelling of ozone mass-transfer through non-porous membranes for water treatment. *Water* **2017**, *9*, 452.
36. Bader, H.; Hoigné, J. Determination of ozone in water by the indigo method. *Water Research* **1981**, *15*, 449-456.

37. Bader, H.; Sturzenegger, V.; Hoigné, J. Photometric method for the determination of low concentrations of hydrogen peroxide by the peroxidase catalyzed oxidation of n,n-diethyl-p-phenylenediamine (dpd). *Water Research* **1988**, *22*, 1109-1115.
38. International Organization for Standardization. Iso 9963-1:1994: Water quality -- determination of alkalinity -- part 1: Determination of total and composite alkalinity. 1994.
39. Sander, R. Compilation of henry's law constants (version 4.0) for water as solvent. *Atmospheric Chemistry & Physics* **2015**, *15*, 4399-4981.
40. Dingemans, M.; Dewulf, J.; Van Hecke, W.; Van Langenhove, H. Determination of ozone solubility in polymeric materials. *Chemical Engineering Journal* **2008**, *138*, 172-178.
41. Atchariyawut, S.; Phattaranawik, J.; Leiknes, T.; Jiraratananon, R. Application of ozonation membrane contacting system for dye wastewater treatment. *Sep. Purif. Technol.* **2009**, *66*, 153-158.
42. Stylianou, S.K.; Kostoglou, M.; Zouboulis, A.I. Ozone mass transfer studies in a hydrophobized ceramic membrane contactor: Experiments and analysis. *Industrial & Engineering Chemistry Research* **2016**, *55*, 7587-7597.
43. Von Gunten, U. Ozonation of drinking water: Part i. Oxidation kinetics and product formation. *Water Research* **2003**, *37*, 1443-1467.
44. Buxton, G.V.; Greenstock, C.L.; Helman, W.P.; Ross, A.B. Critical review of rate constants for reactions of hydrated electrons, hydrogen atoms and hydroxyl radicals (·oh/·o−in aqueous solution. *Journal of Physical and Chemical Reference Data* **1988**, *17*, 513-886.
45. Lee, Y.; von Gunten, U. Oxidative transformation of micropollutants during municipal wastewater treatment: Comparison of kinetic aspects of selective (chlorine, chlorine dioxide, ferratevi, and ozone) and non-selective oxidants (hydroxyl radical). *Water Research* **2010**, *44*, 555-566.
46. Elovitz, M.S.; von Gunten, U. Hydroxyl radical/ozone ratios during ozonation processes. I. The rctconcept. *Ozone: Science & Engineering* **1999**, *21*, 239-260.
47. Wenk, J.; von Gunten, U.; Canonica, S. Effect of dissolved organic matter on the transformation of contaminants induced by excited triplet states and the hydroxyl radical. *Environmental Science & Technology* **2011**, *45*, 1334-1340.
48. Katsoyiannis, I.A.; Canonica, S.; von Gunten, U. Efficiency and energy requirements for the transformation of organic micropollutants by ozone, o3/h2o2 and uv/h2o2. *Water Research* **2011**, *45*, 3811-3822.
49. Ferguson, D.W.; McGuire, M.J.; Koch, B.; Wolfe, R.L.; Aieta, E.M. Comparing peroxone and ozone for controlling taste and odor compounds, disinfection by-products, and microorganisms. *Journal - American Water Works Association* **1990**, *82*, 181-191.
50. Phattaranawik, J.; Leiknes, T.; Pronk, W. Mass transfer studies in flat-sheet membrane contactor with ozonation. *Journal of Membrane Science* **2005**, *247*, 153-167.
51. Stylianou, S.K.; Katsoyiannis, I.A.; Ernst, M.; Zouboulis, A.I. Impact of o3 or o3/h2o2 treatment via a membrane contacting system on the composition and characteristics of the natural organic matter of surface waters. *Environ Sci Pollut Res Int* **2018**, *25*, 12246-12255.
52. Stylianou, S.K.; Katsoyiannis, I.A.; Mitrakas, M.; Zouboulis, A.I. Application of a ceramic membrane contacting process for ozone and peroxone treatment of micropollutant contaminated surface water. *J Hazard Mater* **2018**, *358*, 129-135.
53. Acero, J.L.; Von Gunten, U. Characterization of oxidation processes: Ozonation and the aop o3/h2o2. *Journal - American Water Works Association* **2001**, *93*, 90-100.

54. Fu, Y.J.; Qui, H.Z.; Liao, K.S.; Lue, S.J.; Hu, C.C.; Lee, K.R.; Lai, J.Y. Effect of uv-ozone treatment on poly(dimethylsiloxane) membranes: Surface characterization and gas separation performance. *Langmuir* **2010**, *26*, 4392-4399.
55. Graubner, V.-M.; Jordan, R.; Nuyken, O.; Schnyder, B.; Lippert, T.; Kötz, R.; Wokaun, A. Photochemical modification of cross-linked poly(dimethylsiloxane) by irradiation at 172 nm. *Macromolecules* **2004**, *37*, 5936-5943.
56. Fujimoto, K.; Takebayashi, Y.; Inoue, H.; Ikada, Y. Ozone-induced graft polymerization onto polymer surface. *J. Polym. Sci., Part A: Polym. Chem.* **1993**, *31*, 1035-1043.